BINARY MORPHOLOGY AND LOCAL STATISTICS APPLIED TO IRIS SEGMENTATION FOR RECOGNITION

Lauren R. Kennell, Robert W. Ives, Ruth M. Gaunt

Electrical Engineering Department, U. S. Naval Academy
Annapolis, MD 21402-5025

ABSTRACT

One of the first steps in iris recognition is isolating (or *segmenting*) the iris from an image of the subject's eye area. This paper investigates new approaches for locating the pupil (inner) and limbic (outer) boundaries of the iris, namely a binary morphology and "center of mass" technique for the pupil boundary, and a local statistics approach for the limbic boundary. The methodology and results are presented using images from the University of Bath iris database.

Index Terms – Image segmentation, image processing, image edge analysis.

1. INTRODUCTION

The iris is the colored portion of the eye surrounding the pupil. Its textured pattern is distinct from person to person, and distinct from left eye to right eye of the same person. High pattern variability, the stability of an iris over time, and the non-invasiveness of iris imaging make iris recognition a reliable and practical biometric.

Figure 1 is a typical iris image. The only information used in iris recognition are pixels that actually fall within the iris, so the iris must first be segmented from the rest of the image before it can processed for comparison against other irises. Several means have been proposed to perform this segmentation [1]-[5]. In section 2 of this paper we present a binary morphology method using "center of mass" to locate the pupil boundary. In section 3 we describe a use of local statistics to locate the limbic boundary.

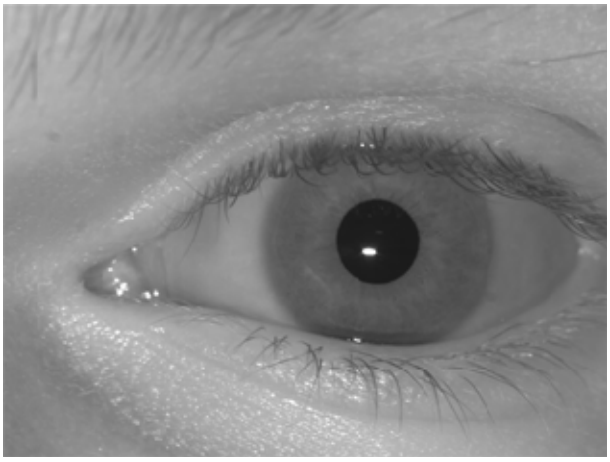

Figure 1: Iris image from the Univ. of Bath database.

Our test images are from the iris database collected at the University of Bath, U.K. [7]. These are 2000 near-infrared (NIR) images from 25 subjects (20 images per eye per subject). They are high resolution (1280x960 pixels), compressed with JPEG-2000 to 0.5 bits/pixel.

We also refer the reader to [6], which presents the authors' earlier results regarding the application of local statistics to both pupil and limbic boundary determination.

2. PUPIL SEGMENTATION

In an iris image, the pupil typically appears as a large dark mass, the largest homogeneous region of dark pixels in the image. Our algorithm takes advantage of this fact by isolating the darker regions of the image to create a binary image, and then performing binary morphology in order to determine which region is actually the pupil. We remark that no assumptions are made as to where the pupil lies within the image. Also, since all of the images we consider are orthogonal (meaning the eye peers straight into the camera, as in Fig. 1), we assume for convenience that pupils (and later, irises also) are circular. The circularity assumption is not actually necessary for binary morphology, but we defer further discussion of the issue until sections 4 and 5. The process to detect the pupil is as follows.

In some cases, because of the illumination conditions or for other reasons, the iris may appear darker than expected so that the boundary between pupil and iris is not very sharp. To sharpen it, we perform adaptive histogram equalization on the image before any segmentation processing begins. In addition, if needed to speed up the processing, we can downsample the image.

Next we use a grayscale threshold to binarize the image; values below the threshold (we use a value of 50 for this database) are changed to 1, those above the threshold

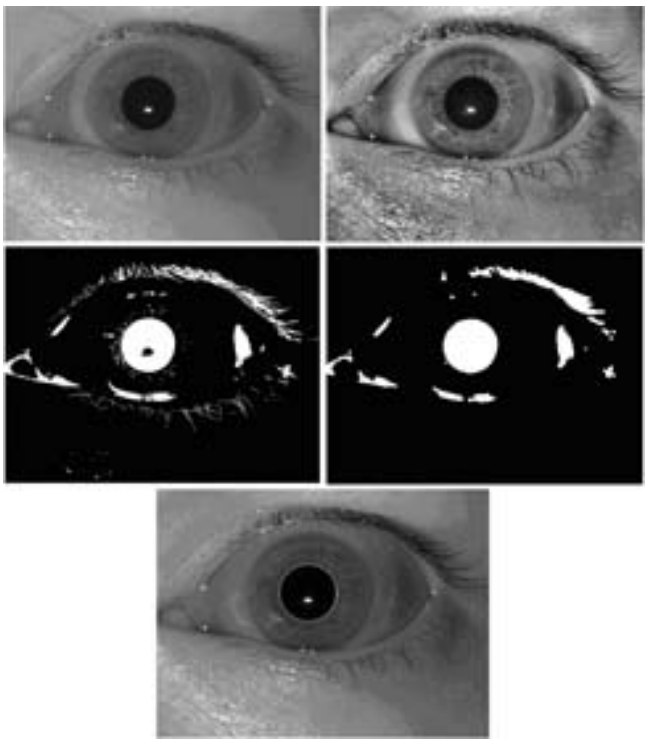

Figure 2: The pupil segmentation process: original image (top left); adaptive histogram equalization (top right); thresholding (second row left); erosion and dilation (second row right); segmentation result (bottom).

become 0. Then we apply binary morphology: (1) a fill, to fill in holes in the masses; (2) an erosion, to get rid of most or all of the noise; and (3) a dilation to restore the mass(es) after erosion. This process is displayed in Fig. 2.

If one mass remains, this is the pupil; if all masses have been removed, then the threshold is raised and we try again. The more complex case is when two or more masses remain, which can result from a dark eyebrow or shadow in the original image. In this case, we use the perimeter and major/minor axis length of each mass to determine whether it is the pupil. An eyebrow or shadow, for instance, usually has a large perimeter, or a very large ratio of major axis length to minor axis length, as compared with a circular pupil. On the other hand, masses from other types of noise have perimeters smaller than that of the pupil.

Once the pupil is determined, we compute its "center of mass," and its radius. (If the pupil is not circular, the radius corresponds to the radius of the smallest circle which encloses it.) We pass the location of the center to the limbic boundary detection algorithm.

3. LIMBIC BOUNDARY SEGMENTATION

The limbic boundary is more difficult to locate than the pupil boundary. One reason is that the transition from the iris to the sclera (the white part of the eye) is more gradual than the transition from the pupil to the iris. Moreover, there may be eyelashes and/or eyelids obscuring portions of the iris. Therefore, to improve the robustness of our method, we adopt the common practice of using the pupil center as an approximate center for the limbic boundary circle. (The two boundaries are in general not exactly concentric, so we will incorporate appropriate adjustments.) The determination of the limbic boundary is otherwise independent from that of the pupil boundary.

The method of local statistics locates the limbic boundary by exploiting statistical properties of the grayscale values within small neighborhoods of pixels. We begin by defining the relevant terms related to statistical data analysis. The *variance* σ^2 on data values X is defined by

$$\sigma^2 = E(X - \overline{X})^2, \tag{1}$$

where E is the expectation operator and $\overline{X}$ is the mean. The standard deviation is σ, the square root of the variance. We also define the *kurtosis*:

$$\kappa = \frac{E\left(X - \overline{X}\right)^4}{\sigma^4}. \tag{2}$$

Kurtosis is a measure of how peaked the data is. The kurtosis of a standard normal distribution of values (σ = 1.0) is 3.0, and distributions that are "flatter" and less prone to outliers have kurtosis less than 3.0 while those distributions that are more peaked and more prone to outliers have kurtosis greater than 3.0.

Returning to Fig. 1, we consider small (overlapping) neighborhoods of pixels. Neighborhoods lying within areas of homogeneous texture, say inside the pupil or sclera, often have relatively uniform grayscale values. However, the iris has a more mottled appearance, so that neighborhoods lying within the iris should contain grayscale values with different local statistical properties. Likewise, neighborhoods overlapping the pupil or limbic boundary should have statistical properties distinct from the interior of the pupil, iris, or sclera.

Experimentally we have found that the local kurtosis was the best statistical parameter for locating the limbic boundary. (By way of comparison, in [6] we used the local standard deviation for locating the pupil boundary.) We use the local kurtosis to create a new image, Fig. 3, as follows: each pixel in Fig. 3, say at row m and column n, reflects the kurtosis value of the 5x5 pixel neighborhood centered at row m, column n in the original image.

Observe that the grayscale values near the limbic boundary are relatively stable in small neighborhoods: locally they are more or less uniformly gray, as opposed to the salt-and-pepper appearance elsewhere. Unfortunately, the relevant pixel values at the boundary are not sufficiently uniform (over various sections of the boundary and across different images) to allow us to simply extract pixels close to a certain value. Instead we create the binary image in Fig.

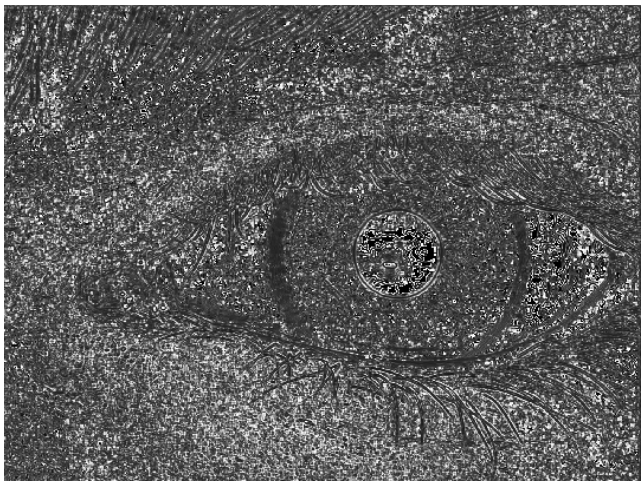

Figure 3: Local kurtosis image.

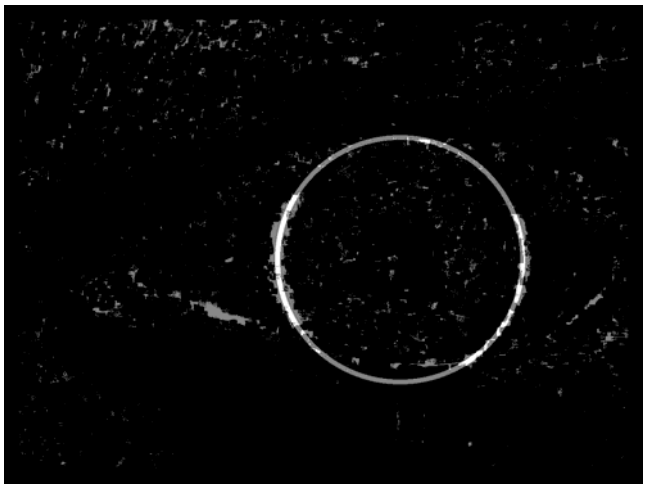

Figure 5: Best-fit annulus overlaid with Figure 4.

4 using another 5x5 window: we assign a value of 1 (white) to pixels for which kurtosis values within a 5x5 neighborhood vary by no more than half the standard deviation over all values in Fig. 3. Although this leaves us with a fair amount of noise, the limbic boundary is easily discernable from the two white arcs.

Now, partly for the sake of processing speed, we use our information about the pupil center. The pupil is sometimes off-center relative to the iris, being slightly closer to the nose. Thus it makes sense to consider multiple possible centers for the limbic boundary. In addition to the pupil center, we consider the pupil center shifted by 5 pixels and 10 pixels to either the left or right, away from the nose. For each center, we generate a family of overlapping concentric annuli, all having a width of 10 pixels (the outer radius minus inner radius), and with the radii increasing in increments of 8. Finally, the limbic boundary (see Fig. 5) is taken to be the annulus containing the highest percentage of ones (white) when "overlaid" with the image in Fig. 4. (Actually, the annulus has width, so we arbitrarily declare the limbic boundary to be its outer edge. We could just as well use the inner edge or the middle.) The final segmentation of the iris image from Fig. 1 is shown in Fig. 6. Further processing, such as edge detection, can then be applied to further remove noise such as eyelashes or eyelids.

A few remarks are in order. First, the neighborhood sizes, the factor 1/2 multiplied against the standard deviation, the annuli widths, the increments of the radii, and the adjustment to the limbic circle center are all of course somewhat arbitrary. Moreover, the location of the limbic boundary is somewhat subjective. For these reasons we make no claim that we have determined the optimal parameters for every user or database. This is actually an advantage, since the parameters can be easily adjusted to prioritize speed or precision, and adjusted according to the properties of a particular camera.

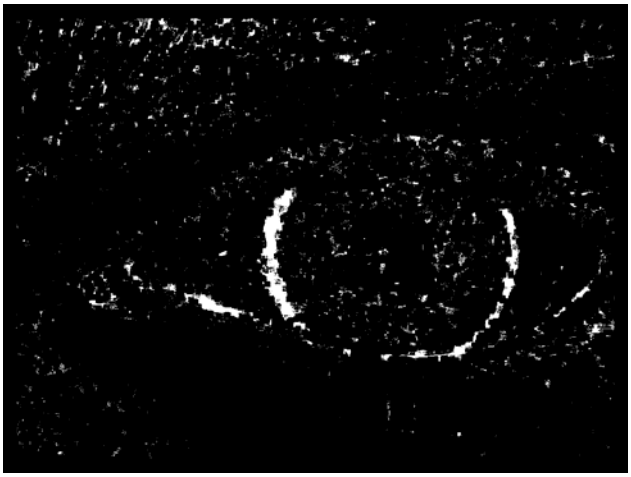

Figure 4: Binary image derived from kurtosis image.

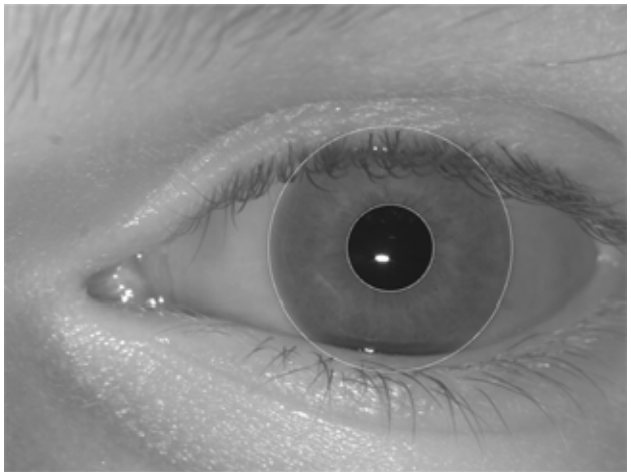

Figure 6: Segmentation result for Figure 1.

4. RESULTS AND CONCLUSIONS

The pupil center was determined correctly in approximately 98.7% of the University of Bath images. The radius was more problematic, because it is fairly common (approximately half of the Bath images) for the pupil to be slightly oblong, even when the person is looking directly at the camera. The pupil segmentation was correct in about 96% of images with a round pupil; in the rest of those images, the size of the pupil was overestimated by varying amounts. For images with oblong pupils, the diameter of the boundary circle corresponded in nearly all cases to the length of the major axis. Thus the pupil boundary circle enclosed a small section of the iris.

The computation of the limbic boundary turned out to be very robust: as long as the pupil *center* was located more or less correctly (even if the pupil was not round), there were no major errors in the limbic boundary. This was true even when eyelashes and eyelids obscured a significant portion of the top and/or bottom of the iris, because the limbic boundary arcs as in Fig. 4 are strong enough to ensure that a good annulus is easy to identify.

The minor errors that occurred are as follows: in a small number of images the limbic boundary excluded a small amount of the iris. In about 75-125 images the boundary enclosed a slight amount of the sclera. These errors can occur, for example, when the limbic center shift is too small. This error is significantly reduced if we allow for larger shifts, for instance 15 or 20 pixels, and also allow for vertical shifts. Another means to reduce inclusion of the sclera is to choose the limbic boundary to be the inner edge of the annulus in Fig. 5. However, in doing so, one can exclude some iris pixels which fall outside that edge.

All in all, the limbic boundary is somewhat subjective, and the definitions of "error" and "significant error" are likewise subjective. When the limbic boundary was not where an observer would place it, the amount of enclosed sclera (or missing iris) was in each case, small.

5. FURTHER REMARKS

The binary morphology process does not require the pupil to be circular; the pupil mass we produce is, in general, the actual shape of the pupil. We enclosed the pupil in a circle at the end of the morphology process to eliminate some segmentation errors which arose from specular reflection (glare spots) near the edge of the pupil. We are currently investigating adjustments to the morphology technique which eliminate glare spots without resorting to a circularity model.

A related area of investigation is the application of morphology and local statistics to segmentation of non-orthogonal iris images. This would certainly require a non-circular model (or better, a model-free approach) for both the pupil and limbic boundary segmentation.

Another area of continuing work regards processing speed: this segmentation algorithm was written for MATLAB, and we are in the process of converting to C. For iris recognition to perform well, it is desirable that the entire process (i.e. image capture, segmentation, feature extraction, and comparison against a database) take at most a few seconds.

6. REFERENCES

[1] J. Huang, Y. Wang, T. Tan, and J. Cui, "A new iris segmentation method for recognition," *Proceedings of the 17th International Conference on Pattern Recognition, 2004 (ICPR 2004)*, Vol. 3, pp. 554-557, Aug. 2004.

[2] W. Kong and D. Zhang, "Accurate iris segmentation based on novel reflection and eyelash detection model," *Proceedings of the 2001 International Symposium on Intelligent Multimedia, Video and Speech Processing*, pp. 263-266, May 2001.

[3] Q. Tian, Q. Pan, Y. Cheng and Q. Gao, "Fast algorithm and application of Hough transform in iris segmentation," *Proceedings of the 2004 International Conference on Machine Learning and Cybernetics*, Vol. 7, pp. 3977-3980, Aug. 2004.

[4] A. Bachoo and J. Tapamo, "A segmentation method to improve iris-based person identification," Proceedings of the 7th AFRICON Conference, Vol. 1, pp. 403-408, Sept. 2004.

[5] J. Daugman, "High Confidence Visual Recognition of Persons by a Test of Statistical Independence," *IEEE Transactions on Pattern Analysis and Machine Intelligence*, Vol. 15, No. 11, pp. 1148-1161, 1993.

[6] Robert W. Ives, Lauren R. Kennell, Ruth M. Gaunt and Delores M. Etter, "Iris segmentation for recognition using local statistics," *Proceedings of the 39th Annual Asilomar Conference on Signals, Systems, and Computers*, in press.

[7] University of Bath, U.K. Iris Image Database, http://www.bath.ac.uk/elec-eng/pages/sipg/irisweb.